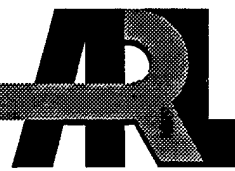


ARMY RESEARCH LABORATORY



Spectroscopic Determination of Impact Sensitivities of Explosives

by K. L. McNesby
and C. S. Coffey

ARL-TR-1323

March 1997

DTIC QUALITY INSPECTED 2

Approved for public release; distribution is unlimited.

19970324 063

The findings in this report are not to be construed as an official Department of the Army position unless so designated by other authorized documents.

Citation of manufacturer's or trade names does not constitute an official endorsement or approval of the use thereof.

Destroy this report when it is no longer need. Do not return it to the originator.

Army Research Laboratory

Aberdeen Proving Ground, MD 21005-5066

ARL-TR-1323

March 1997

Spectroscopic Determination of Impact Sensitivities of Explosives

K. L. McNesby

Weapons and Materials Research Directorate, ARL

C. S. Coffey

Naval Surface Warfare Center

Abstract

A simple theory is developed that predicts impact sensitivities in crystalline explosives from vibrational spectra measured at room temperature. The theory uses Raman spectra of energetic materials to construct vibrational energy level diagrams, which are then used as input for a model designed to calculate the rate of energy transfer from phonon and near-phonon vibrational energy levels to higher energy vibrational levels. Energy transfer rates are determined using Fermi's Golden Rule, and results from simple theories of near-resonant energy transfer. The application of the theory and model, using Raman spectra of seven different neat explosive samples, gives results in good agreement with results of drop weight impact tests.

ACKNOWLEDGMENTS

The authors wish to thank Professor Dana Dlott for a critical review of the original manuscript and for several helpful discussions that corrected several errors. The authors would also like to thank Drs. Betsy Rice and Martin Miller of the U.S. Army Research Laboratory (ARL) and Dr. Sam Trevino of the National Institute of Standards and Technology for helpful discussions on the subject matter in this report.

INTENTIONALLY LEFT BLANK.

TABLE OF CONTENTS

	<u>Page</u>
ACKNOWLEDGMENTS	iii
LIST OF FIGURES	vii
LIST OF TABLES	ix
1. INTRODUCTION	1
2. IMPACT INITIATION MODEL	3
3. EXPERIMENTAL	5
4. BACKGROUND	5
5. QUALITATIVE EVALUATION OF IMPACT SENSITIVITIES	7
6. ENERGY TRANSFER MODEL	8
7. RESULTS AND DISCUSSION	12
8. CONCLUSION	15
9. REFERENCES	27
DISTRIBUTION LIST	29
REPORT DOCUMENTATION PAGE	37

INTENTIONALLY LEFT BLANK.

LIST OF FIGURES

<u>Figure</u>	<u>Page</u>
1. An example of a typical drop weight test apparatus	18
2. Typical results of an energy-to-ignition test, showing initiation occurring early in the impact event	18
3. A schematic of the load-to-shear process in a crystalline energetic material	19
4. Vibrational structure of the bulk solid (left) and of an individual molecular constituent of the bulk solid (right)	20
5. Simple diagram of the experimental apparatus used in these experiments	21
6. The FT-Raman spectra of β -HMX and of γ -HMX. The signal-to-noise ratio in the spectrum of γ -HMX is lower than that of β -HMX, partially due to the lower density of γ -HMX	22
7. An energy level diagram for β -HMX constructed from the spectrum shown in Figure 6. Arrows indicate transitions from the phonon manifold to the internal vibration manifold for which the energy mismatch is less than 10 cm^{-1} . Impact test results indicate β -HMX to be less sensitive than γ -HMX	22
8. An energy level diagram for γ -HMX constructed from the spectrum in Figure 6. Arrows indicate transitions from the phonon manifold to the internal vibration for which the energy mismatch is less than 10 cm^{-1} . Impact test results indicate γ -HMX to be more sensitive than β -HMX	23
9. Division of vibrational energy levels within a molecule into phonon and internal vibration manifolds. Following perturbation by impact, energy is transferred from the phonon manifold to the internal vibration manifold	23
10. Dependence of the unimolecular rate constant on energy mismatch ΔE for vibrational intramolecular energy transfer. Dashed line is the product of a Lorentzian line shape ($\text{HWHM} = 5\text{ cm}^{-1}$) and an approximation to the density of states typical to crystalline explosive materials. The smooth line is the function used in the calculations reported in this paper.	24

<u>Figure</u>	<u>Page</u>
11. The 10-level system used to test the model for vibrational energy transfer in solids. Arrows indicate relative rates, based on energy mismatch, ΔE , for several transitions	24
12. Changes in deviation from equilibrium population, following an initial perturbation, for a phonon manifold level (mode 1, level 4, in Figure 11) and an internal vibration manifold level (mode 3, level 1, in Figure 11). The two levels have similar energies ($\Delta E < 5 \text{ cm}^{-1}$)	25
13. Change in phonon manifold energy (joules) as a function of time after perturbation, for 10-level systems that differ in the number of levels with favorable energy mismatch, ΔE , between phonon manifold energy levels and energy levels within the internal vibration manifold. The rate constant for resonant intramolecular energy transfer is taken to be $1 \times 10^{13} \text{ sec}^{-1}$ (see text)	25
14. Change in phonon manifold energy (joules) as a function of time after perturbation for the seven explosive materials examined in this report. The rate constant for resonant intramolecular energy transfer is taken to be $1 \times 10^{13} \text{ sec}^{-1}$ (see text)	26
15. Experimentally measured impact sensitivities plotted against the initial change (first 100 fs) in energy of the phonon manifold following the shear-dislocation	26

LIST OF TABLES

<u>Table</u>		<u>Page</u>
1. A Comparison of Measured Raman Shift Frequencies for Neat RDX, and a Density Functional Theory Calculation for a Single Molecule of RDX		16
2. Vibrational Energies (cm^{-1}) of Levels Which Make Up the Three, 10-Level Systems Shown in Figure 13. The First Two Columns in Each Distribution Belong to the Internal Vibration Manifold		17
3. The Seven Explosive Samples Analyzed in This Report, and Experimentally Determined Impact Sensitivities		17

INTENTIONALLY LEFT BLANK.

1. INTRODUCTION

One of the simplest and oldest tests used to determine relative sensitivities of explosives and propellants is the drop weight impact test [1]. Although there are many variations of the test, in general, all such tests involve dropping a weight from various heights onto a small amount of explosive or propellant and determining the minimum drop height that causes the material to react. Typical experimental parameters use tens of milligrams of explosive or propellant and drop a several kilogram weight from several to hundreds of centimeters in height [2]. Results are reported in terms of Go-No Go, where a Go may range from an explosion to a smoldering deflagration. An example of a typical drop weight test apparatus is shown in Figure 1.

Results from an impact test designed to measure the energy transferred to the sample show that for sensitive explosives initiation occurs early in the impact event [2], when there is a relatively small decrease in the velocity of the impactor. Typically, results show that ignition of a 50-mg explosive sample occurs when the change in kinetic energy of the impactor ($V_0 > 10$ m/s) is on the order of a few joules, and that initiation occurs from several to tens of microseconds after the impactor comes in contact with the sample [2], when the velocity of the impactor has decreased by just a few percent (see Figure 2).

Assuming a heat capacity [3], C_p , of the sample at room temperature similar to the explosive RDX (0.3 cal/gramK) and uniform distribution of 2 J of energy throughout a 50-mg sample, the change in sample temperature, $\Delta T = \Delta E/C_p$, for the typical test just described is approximately 31 K. Since this temperature rise is insufficient to initiate reaction in practically all energetic materials, the kinetic energy of the impactor, for a Go event, must be localized over a small fraction of the entire sample. From this it follows that, for materials of differing impact sensitivity, the volume of material into which the impact energy is distributed determines the impact sensitivity. Some current theories of impact sensitivity [4] postulate that initiation is due to energy dissipation and localization that takes place during plastic deformation and the ability of the material to shear along certain axes [5]. For these theories, rates of intramolecular energy transfer are secondary within the molecules making up the molecular crystal, since the volume into which the impact energy is

deposited is sufficiently small that the temperature rise of the material within the perturbed volume is several times the decomposition temperature. If low-energy impact initiation is such a thermal process, a measurement of the ability of a series of energetic materials to form shear bands for a given application of force should correlate well with measured impact sensitivities. To our knowledge, no measurement of this type has been made.

Another possible factor contributing to low-energy impact initiation is that the rate at which energy is transferred from the impact event into vibrational modes of the energetic material influences the onset of chemistry. If we suppose that the shear volume for most crystalline energetic materials is about the same for a given impact event, and that thermal equilibrium is always maintained during the impact event, then sensitivities should track according to decomposition temperatures. This is not the case. Since rates of energy transfer in molecular crystals are sufficiently fast [6] that thermal equilibrium should be maintained throughout a low-energy impact event, in order for energy transfer rates to play a role in determining impact sensitivity, there must be a mechanism that allows for deviations from thermal equilibrium during or immediately following the impact event.

For significant deviation from thermodynamic equilibrium to occur following a perturbation, the perturbation must be faster than those processes that maintain the statistical energy distribution within a molecule or collection of molecules. In crystalline materials, thermal energy initially excites the lowest energy lattice and molecular vibrations and is rapidly equilibrated throughout the full vibrational mode structure of the molecule [7]. Lattice and low-energy molecular vibrations in molecular crystals have frequencies near 10^{12} s^{-1} . This means that for the typical impact test mentioned previously, 10^6 low-energy vibrations occur per microsecond for the duration of the energy transfer from impactor to the affected volume of the explosive. With regard to deviations from thermal equilibrium, energy transfer of 2 J from impactor to explosive occurring over 1 μs is similar to slow heating of the explosive over much longer time scales. The conclusion is that direct coupling of mechanical energy from impactor collision into the vibrational modes of the explosive occurs too slowly to cause significant deviation from thermal equilibrium.

We propose a mechanism that takes the slow impact from the drop weight and directs this energy rapidly into the molecule in a way that leads to significant deviations from thermal equilibrium. In what follows, we develop ideas, based on the Raman spectra of explosive materials, for preferentially redistributing energy from impact into vibrational modes that lead to the onset of chemistry.

2. IMPACT INITIATION MODEL

The first part of the mechanism we propose for impact initiation of a crystalline energetic material involves a load-to-shear event. During a low-velocity impact, a pressure load is created on the crystal. Because the load is not distributed isotropically, at a threshold load pressure, the crystal shears (dislocates) along a fracture plane in a way that reduces the pressure load. This is the key to conversion of the slow loading process to a fast process. Essentially, the load buildup causes the crystal to fail (fracture) along a shear plane [8]. This process is illustrated in Figure 3.

For purposes of estimating the shear (dislocation) velocity in molecular crystals, we use the velocity associated with crack growth. For molecular crystals under load, typical values of crack growth velocity [9] are near 10^3 m/s. Velocities of shear (dislocation) bands in the vicinity of the crack decrease rapidly as the distance from the crack front increases [10]. Typical bond lengths [11] in HMX are less than 2×10^{-10} m. This means that during crack and associated shear band formation, near the crack front, molecules in adjacent (fracture or shear) planes are moved, relative to each other, a distance of several bond lengths in hundreds of femtoseconds. This dislocation breaks intermolecular bonds associated with phonon modes in the crystal lattice in a time less than one phonon period of vibration. This results in the dislocation “focusing” the impact energy into the phonon modes of the intact material adjacent to the dislocation in a time less than one period of vibration of the modes being excited. This rapid deposition of energy into the phonon modes of the molecule creates a nonequilibrium distribution of energy among the vibrational modes of the molecule.

The second part of the impact initiation mechanism proposed here depends on the vibrational mode structure of the energetic material. It is generally assumed that a molecular solid is a weakly

interacting system of individual molecules [12]. Vibrations within the solid are usually divided between phonon states, which are vibrations involving the crystal lattice and may not be ascribed to an individual molecule, and internal vibrational states, which are localized on individual molecules. Because the phonon modes are properties of the crystal lattice, they are often referred to as being delocalized and may be visualized as a “bath” of collective states of the entire solid, which lie lower in energy than the individual molecular internal vibrational states (see Figure 4). When energy is deposited into the phonon modes of the crystal, equilibrium is maintained by the transfer of energy from the phonon modes to the internal vibrational modes. The anharmonic coupling of the phonon modes with the internal molecular vibrations, and the excitation of higher lying vibrational modes, is often termed “vibrational up-pumping.” Extensive investigations into this phenomenon have been made by Dlott et al. [13].

In our model, we postulate that the initial excitation (from the shear [dislocation] event) is instantaneously distributed, according to Boltzmann statistics, among the phonon modes and those low-lying vibrational modes with fundamental energies of less than 250 cm^{-1} . This cutoff value was chosen as the maximum value of a fundamental vibration that is highly coupled to the phonon “bath” of the bulk, since phonon densities of states for the energetic materials examined in this report reach a maximum (room temperature) near 100 cm^{-1} . Overtones of these low-lying vibrational modes are also populated. Higher energy fundamental internal vibrational energy levels are not affected by the initial perturbation, since the perturbation occurs on a time scale faster than a period of vibration of the phonon modes excited by the initial shear-dislocation event. Impact sensitivity is determined by how fast energy is transferred from this initially excited group of states, which we call the “phonon manifold,” to internal vibrational states with fundamental vibrational energies up to 700 cm^{-1} (“internal vibrational manifold”). This upper limit cutoff value was chosen because previous work [14] has indicated that energy transfer into vibrational modes between 400 cm^{-1} and 600 cm^{-1} may be rate determining for shock-induced initiation. We propose that the rate of this energy transfer is governed by Fermi’s Golden Rule [15], which states that energy transfer is most efficient for resonant processes. Off-resonance energy transfer is a function of the product of the optical line width of the state being excited and the phonon density of states. Materials that transfer energy to the “internal vibrational manifold” fastest are most sensitive because a greater fraction of the initial energy goes

into vibrational modes that may lead to bond breaking, instead of being distributed among the phonon “bath” of the bulk material. Finally, we use measured Raman spectra to construct energy level diagrams, using a harmonic oscillator approximation, for several explosive materials, and obtain a quantitative measure of impact sensitivity using an energy transfer model based on the ideas presented previously.

3. EXPERIMENTAL

The experimental apparatus has been described previously [16]. Briefly, the equipment employed in these experiments consists of a Bomem DA-8.02 Fourier transform infrared spectrometer, to which a Raman accessory has been added. Incident laser radiation is provided by a Quantronix Series 100 Nd:YAG laser. A simple sketch of the experimental apparatus is shown in Figure 5. Raman-shifted radiation is collected using a back-scattering geometry and is detected, after filtering and interferometer modulation, using a liquid nitrogen-cooled InGaAs detector. All spectra reported here were measured at 4 cm^{-1} resolution using coaddition of 256 scans. The incident laser power at the sample was 400 mW. Neat samples (typically white or yellow powders) of energetic materials were placed in 1-mm i.d. glass capillary tubes, and the Nd:YAG laser focused (spot size approximately 0.5 mm diameter) on the surface of the tube. A near-infrared viewing scope (FJW Optical Systems) was used to visually check laser alignment and also to ensure that the back-scattered radiation was brought to a tight focus at the entrance aperture of the spectrometer. No correction was made to any of the spectra to account for responsivity of the detector, interferometer, or filters used in the experiments. All energetic materials used in these experiments were obtained from in-house sources.

4. BACKGROUND

In calculations to determine impact sensitivity, we use Raman spectra to construct an energy level diagram for the solid explosives used in this study. We use Raman spectroscopy because measurements are well resolved, rapid, *in situ*, nondestructive, and have proven useful in the characterization of explosives [16]. Because energies of vibrational levels are required for the calculations performed here, the best approach is to use values of energies of vibrational levels from

a normal mode analysis of each material under consideration. Unfortunately, calculations for most energetic materials have yet to be performed, especially those calculations which include lattice perturbations to the internal vibrations. Also, application of the theory outlined here on an unknown material cannot rely on information obtained using a normal mode analysis. Additionally, symmetry exclusions [17] prevent Raman spectroscopy from measuring all internal fundamental vibrational transitions. As a measure of the error that might be caused by using a Raman spectrum to construct a vibrational energy level diagram for an energetic material, a density functional theory calculation for a single molecule of RDX was performed [18]. Table 1 shows a comparison (from 100 cm^{-1} to 700 cm^{-1}) of calculated and observed (using Raman spectroscopy) vibrational frequencies for RDX. Although the agreement between observed and calculated values shown in Table 1 is good, the agreement probably would have been better if perturbations from the crystal lattice were included in the calculation. Agreement at higher frequencies (not shown) was always within a few percent of the calculated value. Agreement between all observed and calculated values, with one exception, is always less than 6%, with the one exception by 9%. We believe that the three frequencies not predicted by the calculation are due to lattice modes (149 cm^{-1} , 168 cm^{-1}) or to lattice mode-internal mode coupling (487 cm^{-1}). Of the 14 calculated modes between 100 cm^{-1} and 700 cm^{-1} , 11 were observed in the Raman spectrum, although one mode, calculated at 438 cm^{-1} , was obscured by shoulders, in the measured spectrum, from adjacent peaks.

As an example of the application of the proposed theory, we examine impact initiation in two of the polymorphs of HMX. HMX (Octahydro-1,3,5,7-tetranitro-1,3,5,7-tetrazocine) is an important energetic material used in explosives and propellant formulations. HMX is known to exist in the solid state in four polymorphic forms, referred to as α -, β -, γ -, and δ -HMX [19]. Figure 6 shows the Raman spectrum of β - and γ -HMX shifted from 200 cm^{-1} to $1,600\text{ cm}^{-1}$ relative to the laser line. The spectra are not superimposable, with the most apparent differences in peak position occurring at small Raman shifts. β -HMX is the most commonly encountered form of HMX and is more thermally stable than γ -HMX. β -HMX exists in the “chair” configuration, giving the molecule a center of symmetry, while γ -HMX exists in a “boat” configuration. β - and γ -HMX are well suited for studies of impact initiation since they differ markedly in their impact sensitivity [20]. β -HMX is less sensitive and has an impact sensitivity in the mid-range of most secondary explosive materials

(similar to RDX). On the other hand, γ -HMX has an impact sensitivity more like a primary explosive (similar to Pb styphnate). γ -HMX may be quantitatively prepared from β -HMX by a safe and simple method [20].

5. QUALITATIVE EVALUATION OF IMPACT SENSITIVITIES

In accordance with the previous discussion, Figures 7 and 8 are energy level diagrams constructed, using the spectra shown in Figure 6, of vibrational levels for β -HMX and γ -HMX up to 700 cm^{-1} . Since intramode vibrational energy transfer is assumed to be rapid [21], overtone vibrational levels are included for each transition measured in the spectra. This is an essential feature of the model presented here. Overtone energy levels are assumed to be integral multiples of energies of Raman spectral features below 250 cm^{-1} shift. By assuming that overtone levels are harmonic with the fundamental, we are assuming that energy transfer from a third overtone level is identical to energy transfer involving four quanta of the fundamental. As previously mentioned, it was assumed that the rate limiting step for impact induced chemical reaction involves transfer of energy from the “phonon manifold” to “internal vibration manifold” modes having fundamental energies between 400 cm^{-1} and 700 cm^{-1} . Previous studies [14] have reported a correlation between impact sensitivities and densities of states over this region of the spectrum for several energetic materials. Additionally, intramode energy transfer at energies above these values is believed to occur fast enough so that quasi-equilibrium is always maintained among higher energy states [22]. We propose that the rate of energy transfer from overtones (or equivalently, multiphoton transitions) of “phonon manifold” molecular vibrations to fundamental vibrations belonging to the “internal vibration manifold” plays a role in determining impact sensitivity. These energy transfer processes are assumed to be most efficient when the energy mismatch between donor and acceptor states is minimized. In addition, energy transfer is most favored when the total quantum number change that accompanies the process is minimized [23]. Figures 7 and 8 show that the number of energy transfer processes originating from the “phonon manifold” that have small energy mismatches (arbitrarily chosen as $\Delta E < 10\text{ cm}^{-1}$) for transitions that excite fundamental vibrations between 400 cm^{-1} and 700 cm^{-1} in γ -HMX is double that for β -HMX. This suggests that γ -HMX should be the more impact sensitive of the two polymorphs, in agreement with experiment.

6. ENERGY TRANSFER MODEL

To obtain a quantitative measure of impact sensitivity from measured vibrational frequencies of the crystalline and polycrystalline explosive samples analyzed in this report, it was necessary to construct a numerical model which describes energy redistribution in the solid following a perturbation. The framework of that model is described in the following paragraphs.

As postulated previously, energy from the shear-dislocation event is deposited into the phonon modes and those low-lying internal molecular vibrational modes that have fundamental vibrational energies very near to, or within, the phonon energy “bath.” For this study, it was assumed that internal molecular vibrations with fundamental vibrational frequencies less than 250 cm^{-1} are strongly coupled to the phonon modes and that the initial perturbation (shear-dislocation event) excites these low-lying internal vibrational modes, and their overtones, at the same rate at which the phonon modes are excited. It should be emphasized that this assumption is a main difference between the theory described here and previous theories of vibrational up-pumping [7].

In our model, the energy from the initial perturbation is instantaneously distributed among the energy levels of the “phonon manifold” according to Boltzmann statistics, while the vibrational energy levels outside of the “phonon manifold” remain unaffected. As discussed previously, this occurs because the excitation from the shear-dislocation event is faster than most relaxation processes in the solid. Following the initial, fast perturbation, energy redistribution takes place from the “phonon manifold” to the “internal vibrational manifold.” Vibrational energy transfer can then occur between all levels contained in the model. It should be emphasized that since the initial perturbation is distributed among the energy levels within the “phonon manifold” according to Boltzmann statistics, energy transfer from overtones of fundamental vibrations becomes important. The model essentially simulates microscopic energy transfer between two thermal baths. Sensitivity is determined by the rate at which energy is transferred from the initially excited “phonon manifold” to the “internal vibrational manifold.” This process is shown in Figure 9.

The model employed to describe energy transfer is a simple hybrid of previous theories that have been used with success to describe vibrational energy transfer in gases [15] and vibrational up-pumping in solids [7]. The main idea is that the predominant pathway of energy randomization following a fast perturbation is intramolecular. That is, energy is transferred from one state of a molecule to another state of the same molecule. Impact sensitive materials transfer energy into higher energy fundamentals faster than less sensitive materials. The initially nonstatistical ensemble of excited molecules eventually reaches a distribution described by Boltzmann statistics.

For the model developed here, the vibrational energy transfer rate kinetics are unimolecular. The rate of energy transfer is dependent on the energy mismatch between the two vibrational levels exchanging energy, whether the transfer is intramode or intermode (intramode is favored), and the total quantum number change for the transfer (small changes are favored). These conventions are in keeping with standard theories of vibrational energy transfer in condensed phases and in gases [15].

The first-order rate constant used to describe energy transfer between vibrational levels in the solid is a function of the transfer energy mismatch $\Delta E = E_i - E_j$, where E_i is the energy of the state initially excited, and E_j is the state to which energy is transferred, and T is the temperature of the system. We have chosen the dependence of the rate constant on the transfer energy mismatch to be proportional to $\text{sech}^2(\Delta E/kT)$, in accordance with simple treatments of near-resonant energy transfer in gases [24]. A difference between the function employed here to describe rate constant dependence on energy mismatch and that used for gas phase work is as follows. For gas phase vibrational energy transfer, energy mismatch must be made up by rotations, for which the density of states is near a maximum near zero energy. However, for solid phase transitions, energy mismatch must be made up by phonons, for which the density of states is typically peaked [14] near 100 cm^{-1} . A reasonable function to use for solid-state calculations is the product of the density of states function with a function that describes the optical width of the vibrational energy transition. The resulting function is zero near zero energy mismatch and is slightly broader than the optical line width (see Figure 10). For calculations employed here, an approximation to this product function is used (see Figure 10) that is peaked near zero energy mismatch, in accordance with Fermi's Golden Rule. Additionally, inclusion of resonant energy processes implicitly takes into account higher order phonon processes.

All transition rate constants are first calculated in the exothermic direction, and microscopic reversibility used to calculate the rate constant for the endothermic process. When there is an energy mismatch, ΔE , accompanying energy transfer, energy must be taken up by or supplied by the bulk sample. When this happens, heating and cooling of the sample occurs, changing the equilibrium population distributions. The inclusion of heating is necessary for proper performance of the model.

The calculation of the time dependence of vibrational level populations following perturbation divides the populations in each level into an equilibrium part, N_I^e , and a perturbation part n_I , where the subscript I refers to the level in question. It may be shown [25] that for first order rate processes in multilevel systems, the change in the deviation from equilibrium population of level J is approximated by

$$\Delta n_J = \{ \sum_I K_{IJ}^{I \neq J} [K_{IJ} n_I] - \sum_I K_{JI}^{I \neq J} [K_{JI} n_J] \} \Delta t, \quad (1)$$

where the sum is over all levels (except $I = J$), K_{IJ} and K_{JI} are forward and reverse rate constants, n_I and n_J are deviations from equilibrium population of levels I and J, respectively, and Δt is the time increment. The change in temperature, ΔT , over the same time interval is given by

$$\Delta T = \sum_I (n_I(t) - n_I(t-1)) E_I / C_{PI}, \quad (2)$$

where the sum is over all levels, $n_I(t)$ and $n_I(t-1)$ are population deviations from equilibrium separated by one time element, E_I is the energy of level I, and C_{PI} is the vibrational contribution to the heat capacity of level I.

Figure 11 shows the vibrational energy level structure for a synthetic 10-level molecule used to test the model for vibrational energy transfer outlined previously. Figure 11 shows relative rates of energy transfer for different transitions, where the rate of each transition is dependent upon energy mismatch, ΔE , for the transition being considered.

Figure 12 shows results of calculations, using the model just described, of changes in vibrational level population deviations from equilibrium for the energy level system in Figure 11, following a perturbation of the phonon modes equivalent to raising the “phonon manifold” temperature to 1,000 K. The two levels, from Figure 11, shown in Figure 12 are the highest energy excited “phonon manifold” level (mode 1, level 4) and the “internal vibration manifold” level with energy closest to this “phonon manifold” level (mode 3, level 1). Since these two levels are similar in energy, they equilibrate quickly, and then, as a coupled pair, equilibrate with the remainder of the energy levels in the model system. Since the initial perturbation supplied energy to the model system, the new equilibrium level is caused by the overall increase in system temperature.

Recently, Fried and Ruggiero [14] have calculated rates of upconversion from phonon modes to internal vibrational modes. Rates of energy transfer from phonon modes to internal vibrational modes are calculated as a function of the density of states which may contribute energy during the upconversion process. Since optical measurements of intensities of vibrational transitions yield information on the density of states only for $k \sim 0$ (a limitation when using Raman spectroscopy), Fried and Ruggiero use neutron scattering data to estimate densities of states. The authors then calculate rates of energy transfer from phonon modes into internal vibrational modes which are deemed likely to lead to the onset of reaction (e.g., vibration of the N-N bond in a nitramine). A good correlation is shown between rates of energy transfer from phonon modes to particular frequencies that may lead to onset of reaction.

We have chosen a slightly different approach for several reasons. First, we wished to incorporate our model for low-energy impact initiation by shear/dislocation with an easily accessible diagnostic such as Raman spectroscopy. Second, our model supposes that the phonon modes maintain equilibrium among themselves throughout the upconversion process and that the relaxation process involves equilibration of two energy baths, one composed of the phonon modes and one composed of the internal vibrational energy modes. Also, we believe that the overall internal vibrational mode temperature is rate determining, since at higher energies the internal vibrational modes equilibrate rapidly. Therefore, relating single mode internal vibrational mode temperatures to impact sensitivities may be misleading.

Figure 13 shows the change in energy of the “phonon manifold” as a function of time after initial perturbation, for the 10-level system described previously. The three curves represent vibrational level systems that are identical, except that they differ slightly in the energies of the vibrational levels that make up the “internal vibration manifold.” The three systems have three, one (shown in Figure 11), or zero “internal vibration manifold” energy levels within 10 cm^{-1} of a “phonon manifold” energy level. The energy level structures of the three systems are shown in Table 2.

Figure 13 shows that for the model 10-level vibration system presented previously, the change in energy of the “phonon manifold,” at times immediately following the initial perturbation, is dependent upon the number of near-resonant energy transfer pathways from the “phonon manifold” to the “internal vibration manifold.”

7. RESULTS AND DISCUSSION

To extend the model described previously to evaluation of real explosive samples, energy level diagrams, from measured Raman spectra [26], were constructed for the neat explosives PETN, β -HMX, γ -HMX, TATB, nitroguanidine, RDX, and TNT. Table 3 shows the chemical name for each compound examined in this test and experimentally determined (drop weight test) impact sensitivities [27]. To generate the energy levels used as input to the model calculation, a commercial software peak picking routine (Grams 386, Galactic Industries) was used to select all Raman spectral features between 100 cm^{-1} and 700 cm^{-1} for each of the explosive samples. Each peak selected was assumed to belong to a different mode of internal vibration in the molecule. For each peak measured with an energy less than 350 cm^{-1} , an overtone was generated by multiplying the energy of that peak by integral values, such that overtones up to 700 cm^{-1} were included as input to the model calculation. By this convention, a single spectral peak measured at 100 cm^{-1} would have six overtone levels considered in the calculation.

Once the energy level diagram was constructed, all modes with fundamentals less than 250 cm^{-1} were considered as part of the “phonon manifold,” with all other modes belonging to the “internal vibration manifold.” The initial perturbation then excited all modes with fundamentals less than

250 cm^{-1} , and the overtones associated with each of those modes. The excitation was distributed among these fundamental and overtone levels according to the Boltzmann distribution. The excitation used was an initial heating of the phonon manifold to 1,000 K. Several other, lesser degrees of heating were tried to see if the degree of initial excitation affected the behavior of the model. In each case, the output of the model was independent of the magnitude of the initial excitation, as expected, since first order kinetics are employed in the model.

The first order intramolecular energy transfer rate constant for resonant processes was approximated in the following manner. Measurements [15] of vibrational relaxation of diatomic molecules in inert gas matrices have shown the first order rate constant for processes with an energy mismatch, ΔE , near 100 cm^{-1} to be on the order of $1 \times 10^{10}\text{ sec}^{-1}$. For this work, we have chosen the dependence of the rate constant on the transfer energy mismatch to be proportional to $\text{sech}^2(\Delta E/kT)$. Using this function, an energy transfer process with an energy mismatch of 100 cm^{-1} would have a resonant ($\Delta E = 0$) energy transfer rate constant of $1 \times 10^{13}\text{ sec}^{-1}$. This value for the first order rate constant for resonant energy transfer processes was used throughout the calculations reported here.

Figure 14 shows the change in “phonon manifold” energy as a function of time after initial perturbation, for the seven explosive materials examined for this report. Figure 15 shows a plot of “phonon manifold” energy change during the first 10 fs following the perturbation, calculated using the model developed here, vs. experimentally determined impact sensitivities. The calculated differences between very sensitive (PETN, γ -HMX) and sensitive (RDX, β -HMX) are small, with the differences between the sensitive materials and insensitive materials (TATB, nitroguanidine) much larger. The correlation between results of impact tests for these explosives and calculated rates of energy transfer from the “phonon manifold” of each of the explosives is good. We should note that TATB and nitroguanidine are among the most insensitive of all explosives, and the reported impact sensitivities for these compounds varies in the literature. We chose to use values reported in one of the most used references [27], which reported an impact sensitivity for TATB of 50 N·m, and reported “no reaction up to 49 N·m” for nitroguanidine.

Figure 14 shows that for each of the explosive samples examined in this report, the energy transferred from the “phonon manifold” reaches at least half of its initial value in less than 50 fs. During the shear-dislocation event, only a small fraction of the bulk sample is actually perturbed, with phonons dissipating heat rapidly throughout the bulk material. Phonons travel at approximately the speed of sound in solid materials (generally on the order of several micrometers per nanosecond [28]). Therefore, for the model reported here, dissipation of energy from the phonon manifold to the bulk of the material is much slower than energy transfer from the “phonon manifold” to the “internal vibration manifold.”

There seems to be general agreement that many different physical properties and processes occurring within the solid phase contribute to impact sensitivity [29]. We believe these results show that the number of near-resonant energy transfer processes which can result in energy transfer between the “phonon manifold” and the “internal vibration manifold” of a crystalline explosive material influences low-energy impact sensitivity. These results support the importance of shear-dislocation effects in molecular crystals, allowing a slow event (impact) to rapidly channel energy into specific vibrational modes of the molecule.

The model has several shortcomings, chief among which are that we have not accounted for anharmonicity of vibrational levels, have neglected transition intensities, and have not considered orthogonality of eigenvectors of vibrations in calculating energy transfer rates. We hope to be able to address these limitations in the near future. Additionally, we have not mentioned effect of particle size on sensitivity, although current work in our lab (not presented here) shows correlation between model calculations and impact testing of RDX of particle sizes from $38\text{ }\mu\text{m}$ to several millimeters. Several ways to improve and check the theory are currently being explored. These include calculations of how the lattice perturbs the individual molecule, inclusion of degeneracies and transition intensities in the rate calculations (not included in the current model), inclusion of combination (i.e., three state) transitions, and refinement of the calculation of rate coefficients for near-resonant energy transfer in condensed media. However, even given the shortcomings of the current model, the success of the theory outlined previously in determining impact sensitivities from

room temperature measurements of Raman spectra of crystalline explosives merits further consideration.

8. CONCLUSION

A new mechanism that contributes to the determination of low-energy impact initiation of crystalline energetic materials, based upon transition of a slow event (impact) into a fast event (shear-dislocation), is proposed. The effect of the shear-dislocation event is to deposit energy into a band of molecules adjacent to the shear-dislocation planes faster than energy redistribution processes can randomize that energy. Following this rapid, exclusive perturbation of low-energy modes, the initial rate of energy transfer from these low energy modes into states with higher energy is determined by Fermi's Golden Rule. Results of calculations suggest that this initial rate of energy transfer, from states within a low-energy "phonon manifold" to states within a higher energy "internal vibrational manifold," plays a role in determining impact sensitivities of the explosives examined in this report.

Table 1. A Comparison of Measured Raman Shift Frequencies for Neat RDX, and a Density Functional Theory Calculation for a Single Molecule of RDX

Observed Raman Shift (cm ⁻¹)	Calculated Vibrational Frequency (cm ⁻¹)/ Intensity (KM/Mol)
109	107/0.0074
149	—
168	—
206	209/8.3177
225	229/1.7658
346	325/2.5840
385	371/0.0752
415	403/8.5605
	405/0.6307
Obscured	438/5.8478
462	463/25.9101
487	—
546	579/10.1865
590	588/0.3703
605	609/14.5462
	651/0.6618
668	676

Table 2. Vibrational Energies (cm^{-1}) of Levels That Make Up the Three, 10-Level Systems Shown in Figure 13. The First Two Columns in Each Distribution Belong to the Internal Vibration Manifold

System 1—Level Energies 3 Transitions $\Delta E < 10 \text{ cm}^{-1}$					System 2—Level Energies 1 Transition $\Delta E < 10 \text{ cm}^{-1}$					System 3—Level Energies 0 Transitions $\Delta E < 10 \text{ cm}^{-1}$				
150	280	600	601	602	150	280	600	625	640	150	280	580	625	640
300	560				300	560				300	560			
450					450					450				
600					600					600				

Table 3. The Seven Explosive Samples Analyzed in This Report, and Experimentally Determined Impact Sensitivities

Explosive Material	Impact Sensitivity [27]	Calculated Change in Phonon Energy for First 10 fs Following Shear-Dislocation (J)
PETN (pentaerythrol tetranitrate)	3 N·m	-50.43
γ -HMX (γ -cyclotetramethylene tetranitramine)	est 3 N·m	-51.51
β -HMX (β -cyclotetramethylene tetranitramine)	7.4 N·m	-40.35
RDX (cyclo-1,3,5-trimethylene-2,4,6-trinitramine)	7.4 N·m	-46.85
TNT (trinitrotoluene)	15 N·m	-35.67
TATB (triaminotrinitobenzene)	50 N·m	-12.50
Nitroguanidine	>49 N·m	-09.25

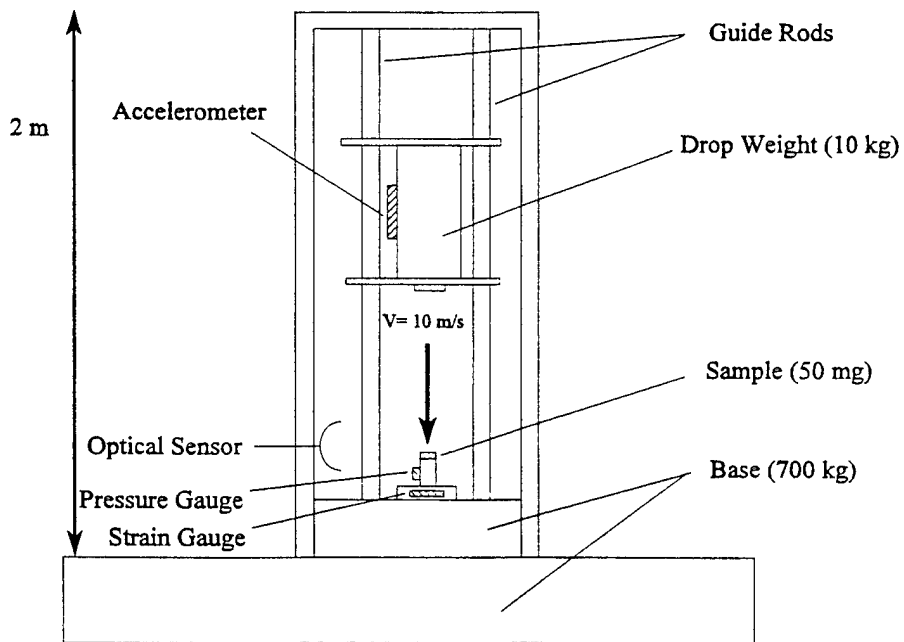


Figure 1. An example of a typical drop weight test apparatus.

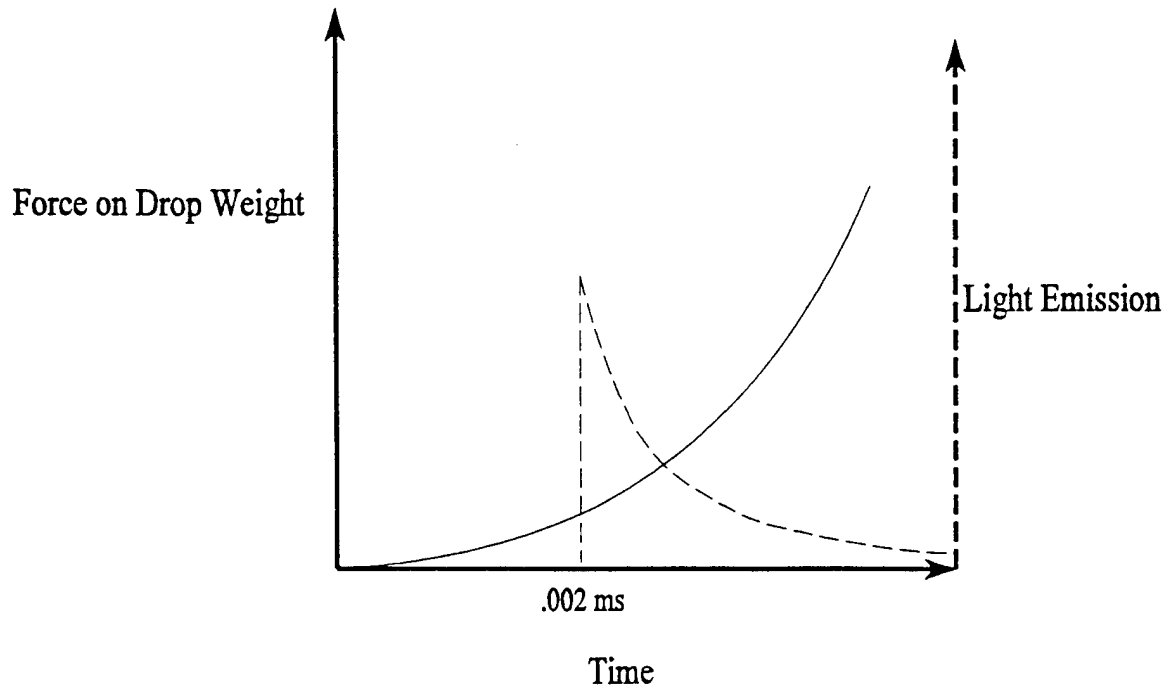


Figure 2. Typical results of an energy-to-ignition test, showing initiation occurring early in the impact event.

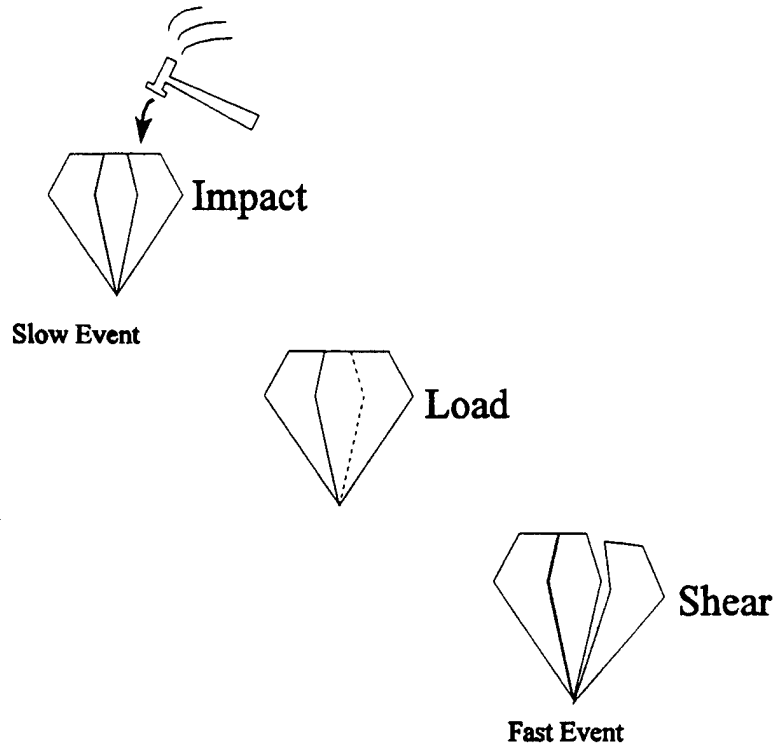


Figure 3. A schematic of the load-to-shear process in a crystalline energetic material.

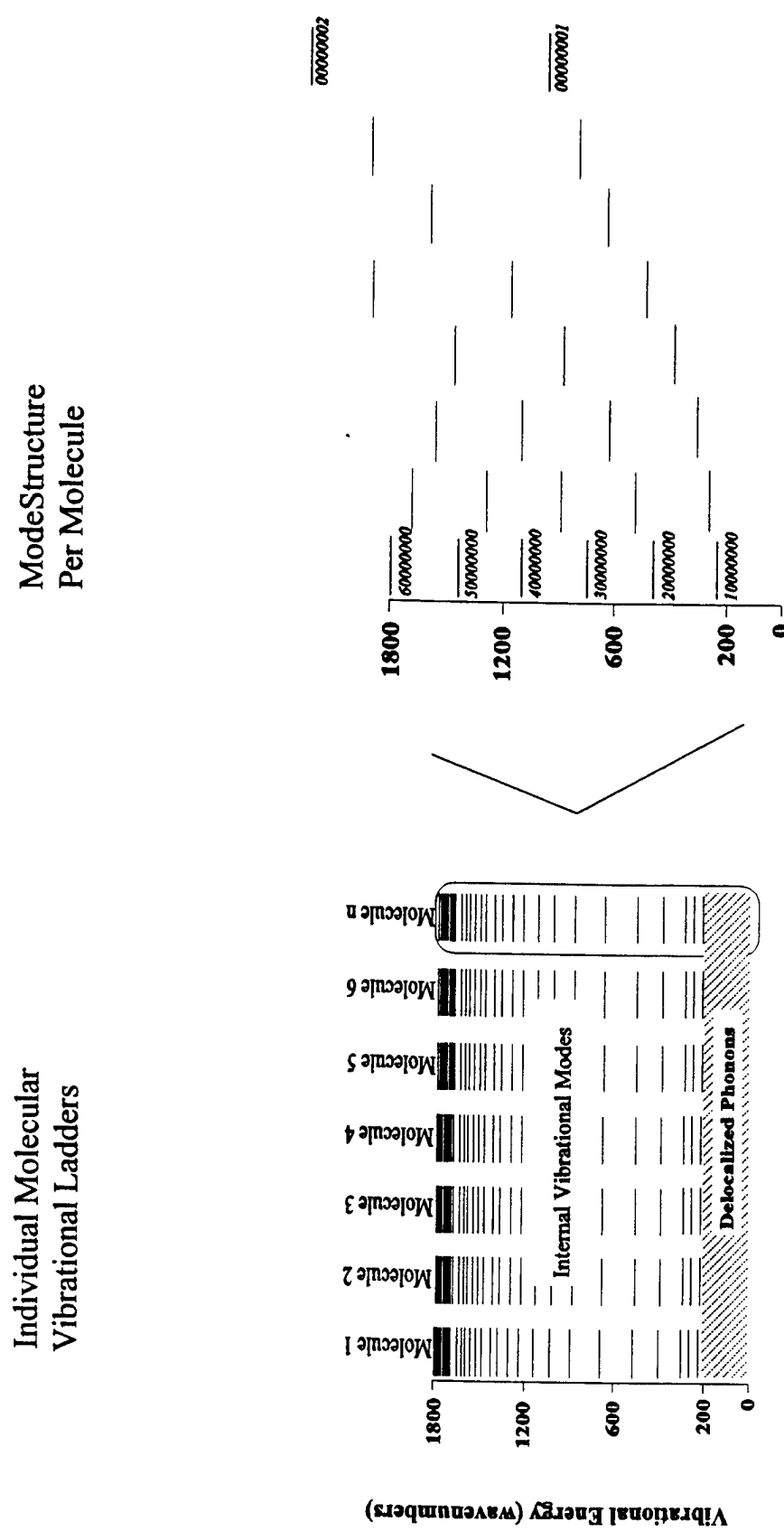


Figure 4. Vibrational structure of the bulk solid (left) and of an individual molecular constituent of the bulk solid (right).

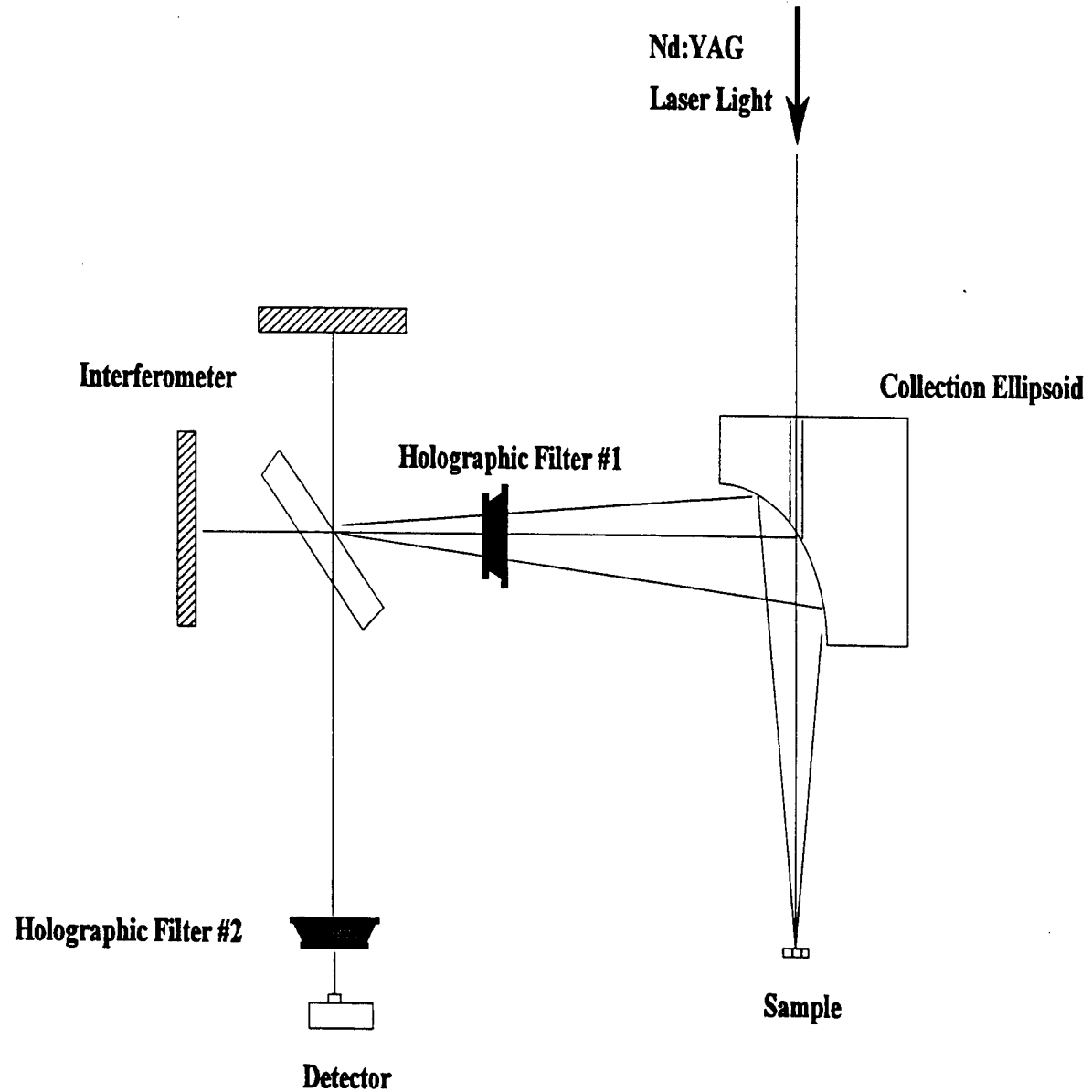


Figure 5. Simple diagram of the experimental apparatus used in these experiments.

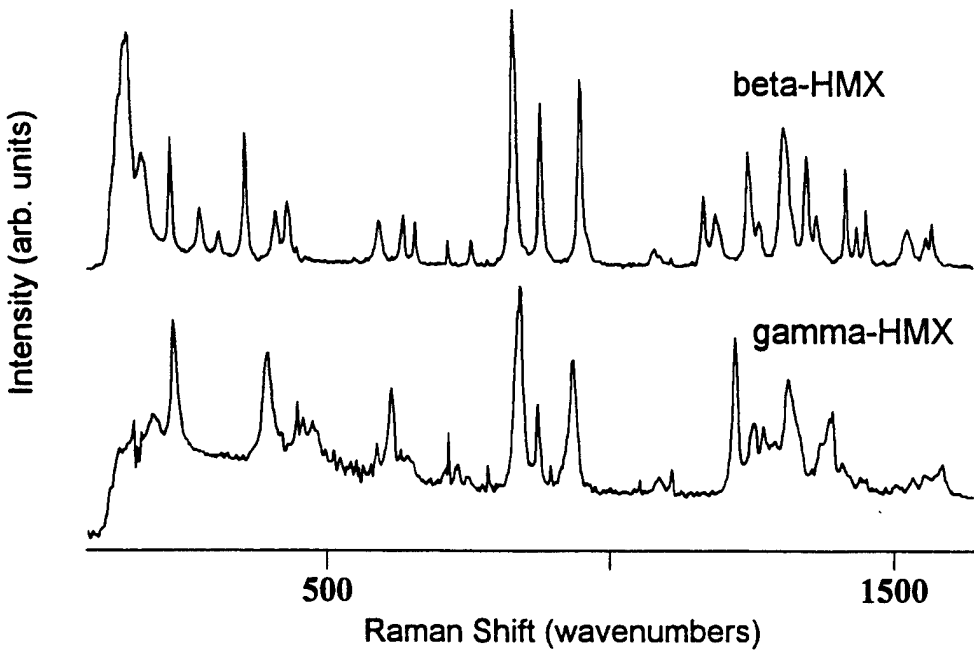


Figure 6. The FT-Raman spectra of β -HMX and of γ -HMX. The signal-to-noise ratio in the spectrum of γ -HMX is lower than that of β -HMX, partially due to the lower density of γ -HMX.

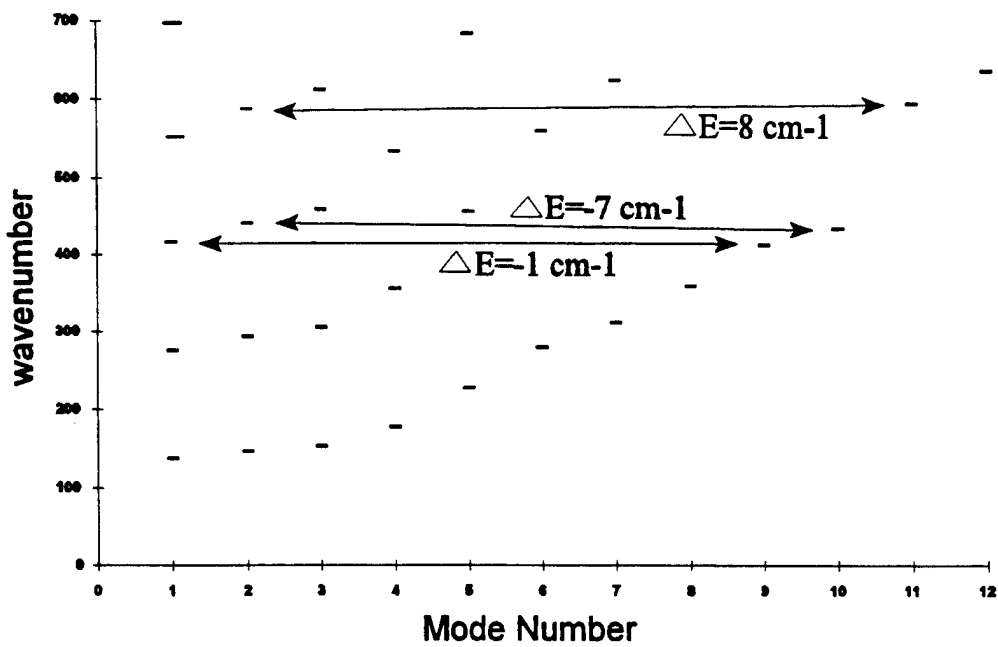


Figure 7. An energy level diagram for β -HMX constructed from the spectrum shown in Figure 6. Arrows indicate transitions from the phonon manifold to the internal vibration manifold for which the energy mismatch is less than 10 cm^{-1} . Impact test results indicate β -HMX to be less sensitive than γ -HMX.

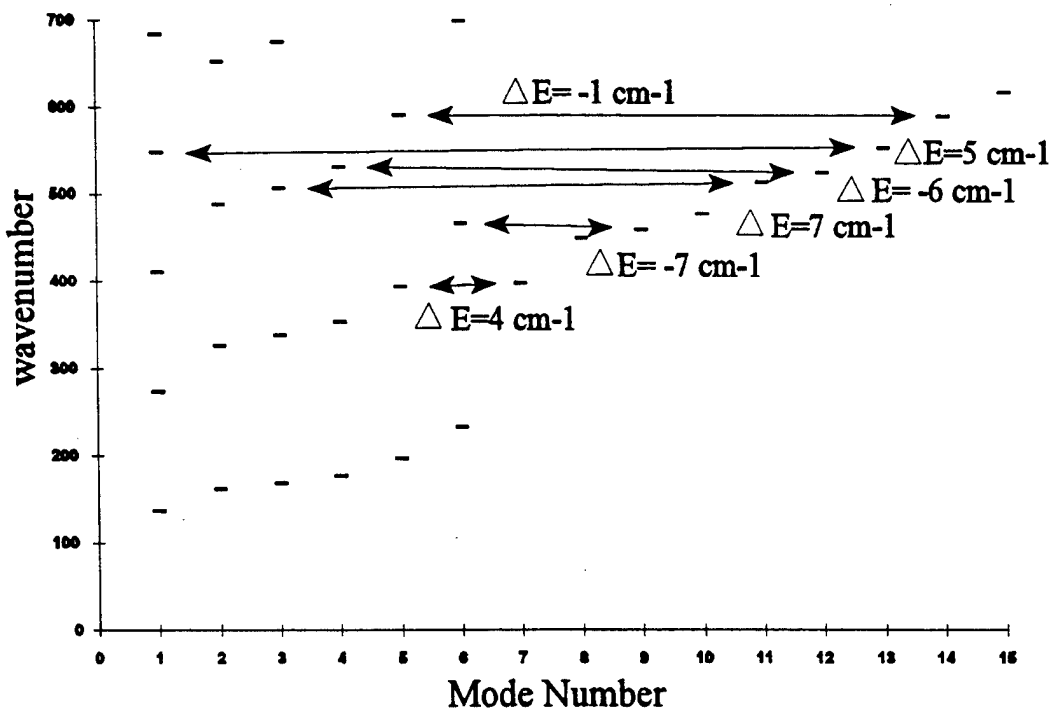


Figure 8. An energy level diagram for γ -HMX constructed from the spectrum in Figure 6. Arrows indicate transitions from the phonon manifold to the internal vibration for which the energy mismatch is less than 10 cm^{-1} . Impact test results indicate γ -HMX to be more sensitive than β -HMX.

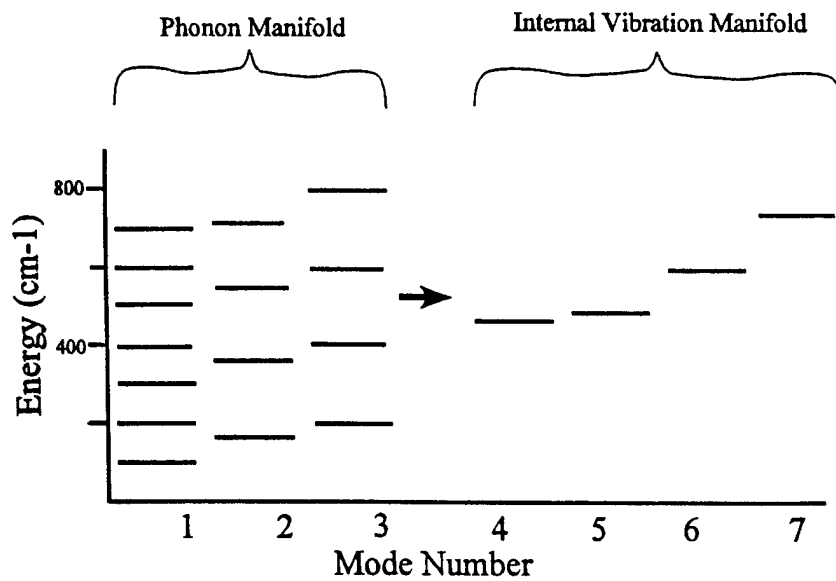


Figure 9. Division of vibrational energy levels within a molecule into phonon and internal vibration manifolds. Following perturbation by impact, energy is transferred from the phonon manifold to the internal vibration manifold.

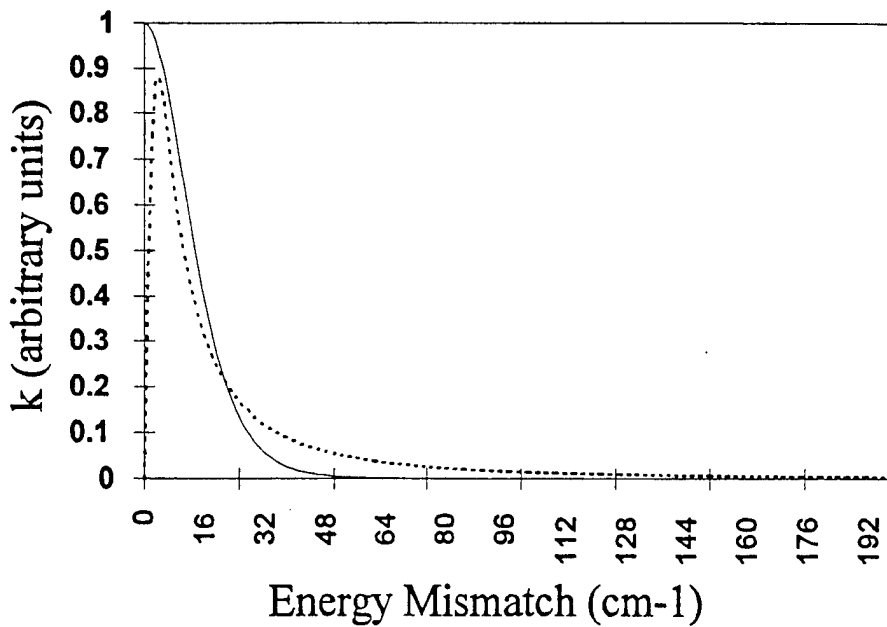


Figure 10. Dependence of the unimolecular rate constant on energy mismatch ΔE for vibrational intramolecular energy transfer. Dashed line is the product of a Lorentzian line shape ($\text{HWHM} = 5 \text{ cm}^{-1}$) and an approximation to the density of states typical to crystalline explosive materials. The smooth line is the function used in the calculations reported in this report.

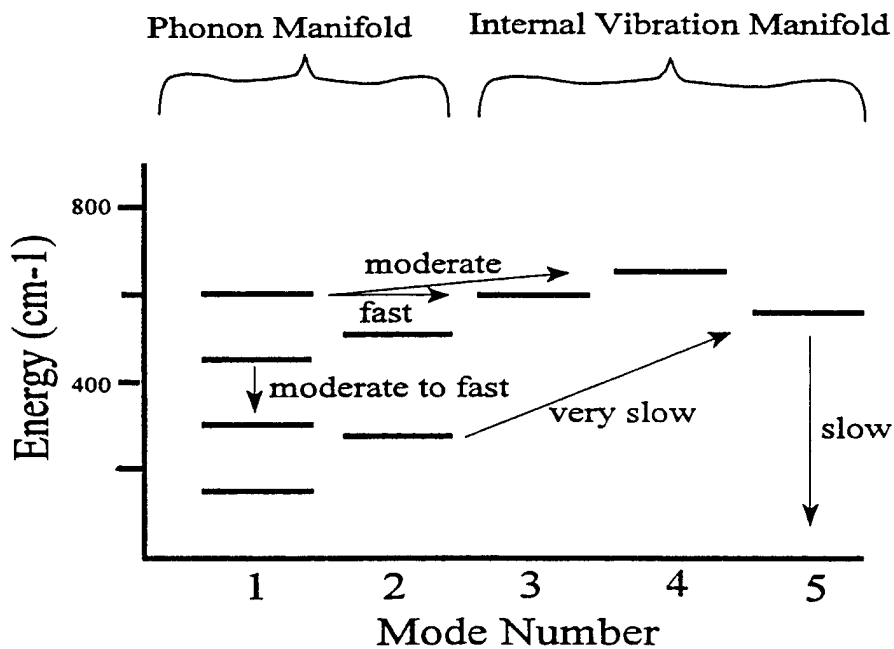


Figure 11. The 10-level system used to test the model for vibrational energy transfer in solids. Arrows indicate relative rates, based on energy mismatch, ΔE , for several transitions.

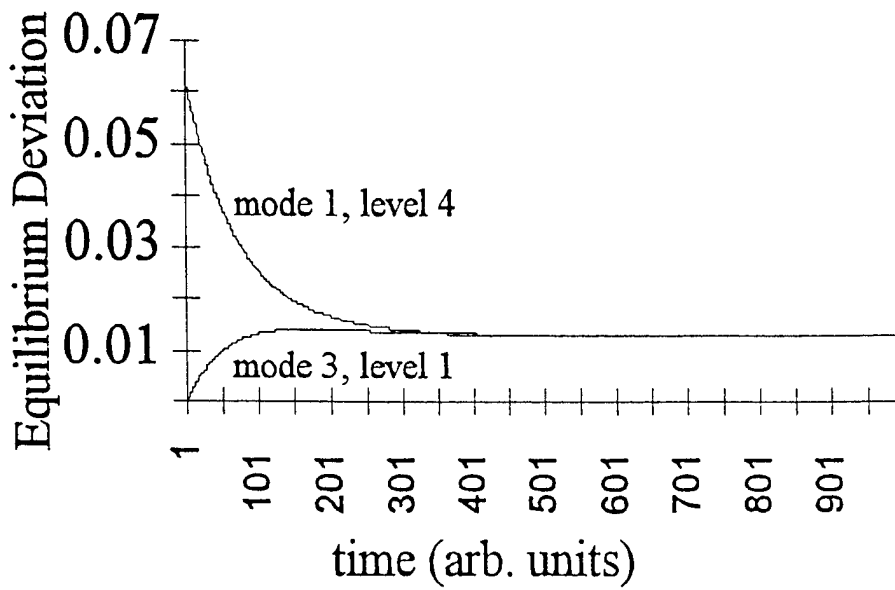


Figure 12. Changes in deviation from equilibrium population, following an initial perturbation, for a phonon manifold level (mode 1, level 4, in Figure 11) and an internal vibration manifold level (mode 3, level 1, in Figure 11). The two levels have similar energies ($\Delta E < 5 \text{ cm}^{-1}$).

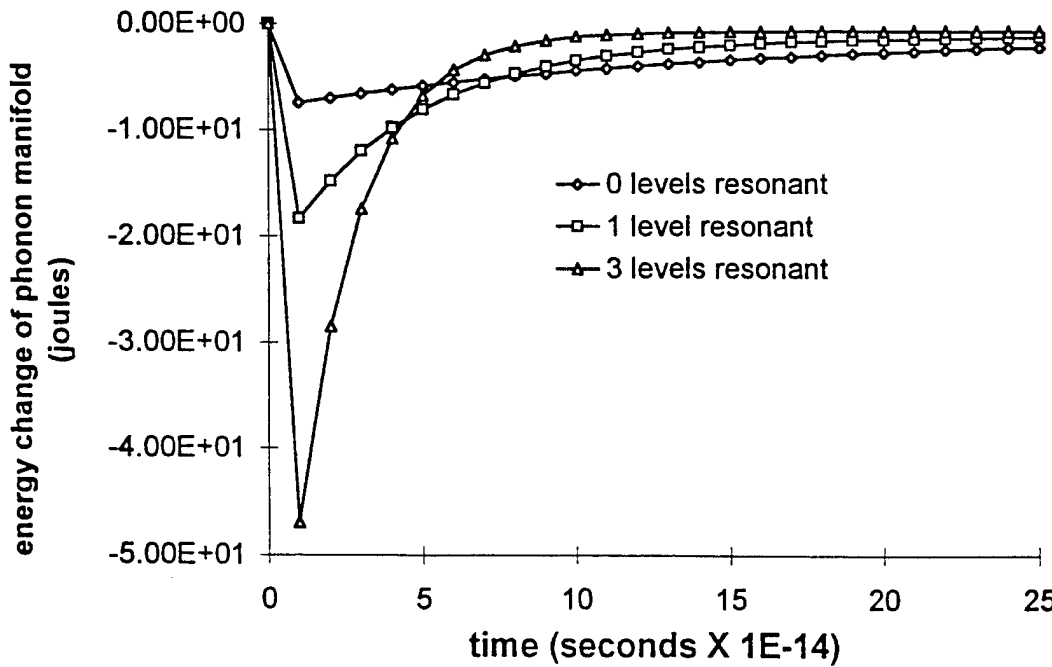


Figure 13. Change in phonon manifold energy (joules) as a function of time after perturbation, for 10-level systems that differ in the number of levels with favorable energy mismatch, ΔE , between phonon manifold energy levels and energy levels within the internal vibration manifold. The rate constant for resonant intramolecular energy transfer is taken to be $1 \times 10^{13} \text{ sec}^{-1}$ (see text).

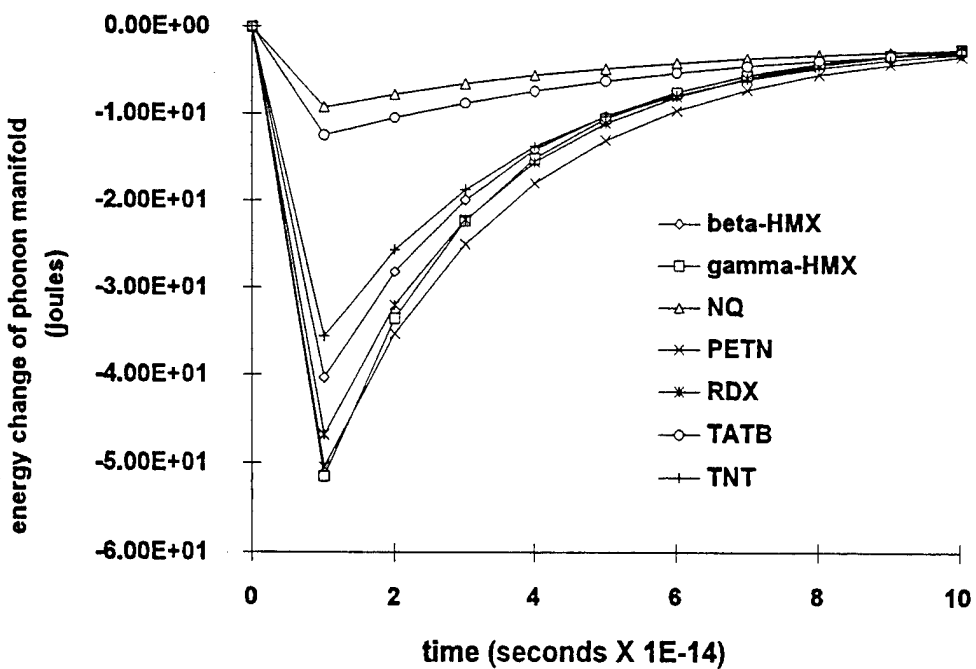


Figure 14. Change in phonon manifold energy (joules) as a function of time after perturbation for the seven explosive materials examined in this report. The rate constant for resonant intramolecular energy transfer is taken to be $1 \times 10^{13} \text{ sec}^{-1}$ (see text).

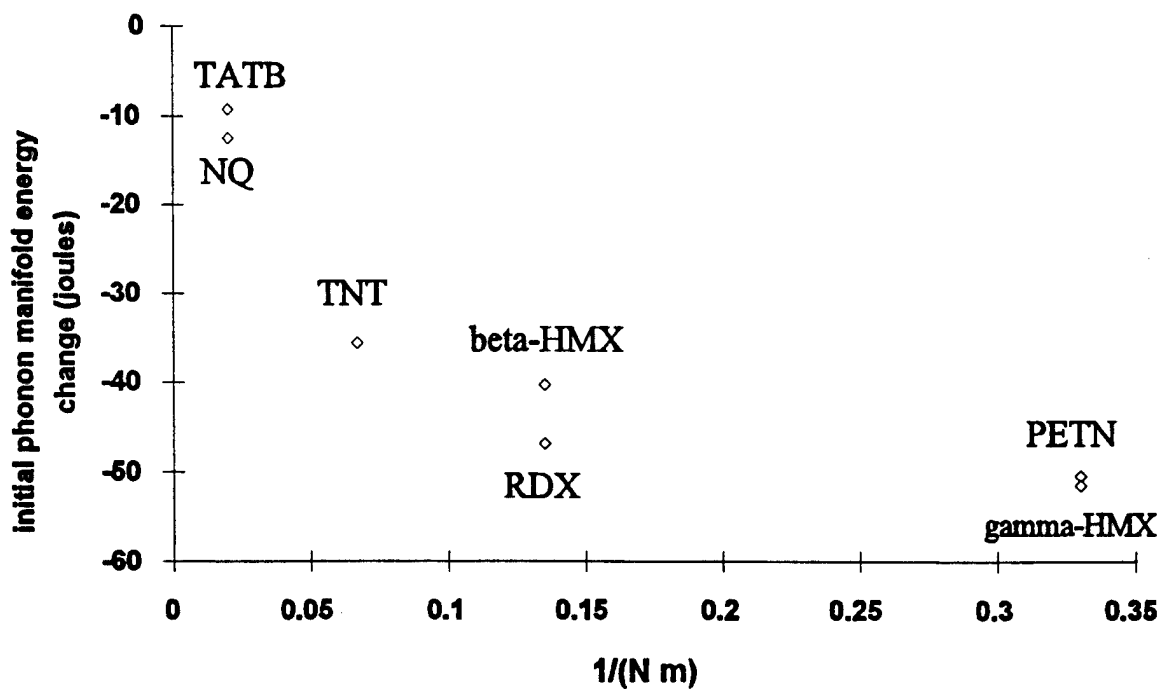


Figure 15. Experimentally measured impact sensitivities plotted against the initial change (first 100 fs) in energy of the phonon manifold following the shear-dislocation.

9. REFERENCES

1. Robertson, R. Trans. Chem. Soc., vol. 18, 1921.
2. Coffey, C. S., and V. F. DeVost. Propellants, Explosives, Pyrotechnics, vol. 20, p. 105, 1995.
3. "CPIA/M3 Solid Propellant Ingredients Manual." Chemical Propulsion Information Agency, The Johns Hopkins University, Columbia, MD, September 1994.
4. Coffey, C. S. "Initiation of Crystalline Explosives by Shock or Impact." Decomposition, Combustion, and Detonation Chemistry of Energetic Materials, Material Research Society Symposium Proceedings, vol. 418, pp. 331–336, Materials Research Society, Pittsburgh, PA, 1996.
5. Dick, J. J. App. Phys. Lett., vol. 44, p. 859, 1984.
6. Hong, X., J. R. Hill, and D. D. Dlott. "Vibrational Energy Transfer in High Explosives: Nitromethane." Decomposition, Combustion, and Detonation Chemistry of Energetic Materials, Material Research Society Symposium Proceedings, vol. 418, pp. 357–362, Materials Research Society, Pittsburgh, PA, 1996.
7. Dlott, D. D., and M. D. Fayer. J. Chem. Phys., vol. 92, p. 3798, 1990.
8. Coffey, C. S., and S. J. Jacobs. J. Applied Physics, vol. 52, p. 6991, 1981.
9. Gazonas, G. A. Mechanics of Materials, vol. 15, p. 323, 1993.
10. Sharma, J., C. S. Coffey, A. L. Ramaswamy, and R. W. Armstrong. "Atomic Force Microscopy of Hot Spot Reaction Sites in Impacted RDX and Laser Heated AP." Decomposition, Combustion, and Detonation Chemistry of Energetic Materials, Material Research Society Symposium Proceedings, vol. 418, pp. 357–362, Materials Research Society, Pittsburgh, PA, 1996.
11. Pauling, L. "The Nature of the Chemical Bond." Ithaca, NY: Cornell University Press, 1960.
12. Kitaigorodskii, A. I. "Molecular Crystals and Molecules." New York: Academic Press, 1973.
13. Chen, S., W. A. Tolbert, and D. D. Dlott. J. Phys. Chem., vol. 98, p. 7759, 1994. Also see A. Tokmakoff, M. D. Fayer, and D. D. Dlott. J. Phys. Chem., vol. 97, p. 1901, 1993, and references contained therein.
14. Fried, L. E., and A. J. Ruggiero. J. Phys. Chem., vol. 98, p. 9786, 1994.
15. Yardley, J. T. "Introduction to Molecular Energy Transfer." New York: Academic Press, 1980.

INTENTIONALLY LEFT BLANK.

<u>NO. OF COPIES</u>	<u>ORGANIZATION</u>
2	DEFENSE TECHNICAL INFO CTR ATTN DTIC DDA 8725 JOHN J KINGMAN RD STE 0944 FT BELVOIR VA 22060-6218
1	HQDA DAMO FDQ ATTN DENNIS SCHMIDT 400 ARMY PENTAGON WASHINGTON DC 20310-0460
1	US MILITARY ACADEMY MATH SCI CTR OF EXCELLENCE DEPT OF MATHEMATICAL SCI ATTN MDN A MAJ DON ENGEN THAYER HALL WEST POINT NY 10996-1786
1	DIRECTOR US ARMY RESEARCH LAB ATTN AMSRL CS AL TP 2800 POWDER MILL RD ADELPHI MD 20783-1145
1	DIRECTOR US ARMY RESEARCH LAB ATTN AMSRL CS AL TA 2800 POWDER MILL RD ADELPHI MD 20783-1145
3	DIRECTOR US ARMY RESEARCH LAB ATTN AMSRL CI LL 2800 POWDER MILL RD ADELPHI MD 20783-1145

ABERDEEN PROVING GROUND

2 DIR USARL
ATTN AMSRL CI LP (305)

<u>NO. OF COPIES</u>	<u>ORGANIZATION</u>	<u>NO. OF COPIES</u>	<u>ORGANIZATION</u>
1	HQDA ATTN SARD TT DR F MILTON PENTAGON WASHINGTON DC 20310-0103	2	COMMANDER US ARMY MISSILE COMMAND ATTN AMSMI RD PR E A R MAYKUT AMSMI RD PR P R BETTS REDSTONE ARSENAL AL 35809
1	HQDA ATTN SARD TT MR J APPEL PENTAGON WASHINGTON DC 20310-0103	1	OFFICE OF NAVAL RESEARCH DEPARTMENT OF THE NAVY ATTN R S MILLER CODE 432 800 N QUINCY STREET ARLINGTON VA 22217
1	HQDA OASA RDA ATTN DR C H CHURCH PENTAGON ROOM 3E486 WASHINGTON DC 20310-0103	1	COMMANDER NAVAL AIR SYSTEMS COMMAND ATTN J RAMNARACE AIR 54111C WASHINGTON DC 20360
4	COMMANDER US ARMY RESEARCH OFFICE ATTN R GHIRARDELLI D MANN R SINGLETON R SHAW P O BOX 12211 RSCH TRNGLE PK NC 27709-2211	2	COMMANDER NAVAL SURFACE WARFARE CENTER ATTN R BERNECKER R 13 G B WILMOT R 16 SILVER SPRING MD 20903-5000
1	DIRECTOR US ARMY RESEARCH OFFICE ATTN AMXRO MCS K CLARK PO BOX 12211 RSCH TRNGLE PK NC 27709-2211	5	COMMANDER NAVAL RESEARCH LABORATORY ATTN M C LIN J MCDONALD E ORAN J SHNUR R J DOYLE CODE 6110 WASHINGTON DC 20375
1	DIRECTOR US ARMY RESEARCH OFFICE ATTN AMXRO RT IP LIB SERVICES P O BOX 12211 RSCH TRNGLE PK NC 27709-2211	2	COMMANDER NAVAL WEAPONS CENTER ATTN T BOGGS CODE 388 T PARR CODE 3895 CHINA LAKE CA 93555-6001
2	COMMANDER US ARMY ARDEC ATTN SMCAR AEE B D S DOWNS PCTNY ARSNL NJ 07806-5000	1	SUPERINTENDENT NAVAL POSTGRADUATE SCHOOL DEPT OF AERONAUTICS ATTN D W NETZER MONTEREY CA 93940
2	COMMANDER US ARMY ARDEC ATTN SMCAR AEE J A LANNON PCTNY ARSNL NJ 07806-5000	3	AL LSCF ATTN R CORLEY R GEISLER J LEVINE EDWARDS AFB CA 93523-5000
1	COMMANDER US ARMY ARDEC ATTN SMCAR AEE BR L HARRIS PCTNY ARSNL NJ 07806-5000		

<u>NO. OF COPIES</u>	<u>ORGANIZATION</u>	<u>NO. OF COPIES</u>	<u>ORGANIZATION</u>
1	AFOSR ATTN J M TISHKOFF BOLLING AIR FORCE BASE WASHINGTON DC 20332	2	PRINCETON COMBUSTION RESEARCH LABORATORIES INC ATTN N A MESSINA M SUMMERFIELD PRINCETON CORPORATE PLAZA BLDG IV SUITE 119 11 DEERPARK DRIVE MONMOUTH JUNCTION NJ 08852
1	OSD SDIO IST ATTN L CAVENY PENTAGON WASHINGTON DC 20301-7100	3	DIRECTOR SANDIA NATIONAL LABORATORIES DIVISION 8354 ATTN S JOHNSTON P MATTERN D STEPHENSON LIVERMORE CA 94550
1	COMMANDANT USAFAS ATTN ATSF TSM CN FORT SILL OK 73503-5600	1	BRIGHAM YOUNG UNIVERSITY DEPT OF CHEMICAL ENGINEERING ATTN M W BECKSTEAD PROVO UT 84058
1	UNIV OF DAYTON RSCH INSTITUTE ATTN D CAMPBELL AL PAP EDWARDS AFB CA 93523	1	CALIFORNIA INSTITUTE OF TECH JET PROPULSION LABORATORY ATTN L STRAND MS 125 224 4800 OAK GROVE DRIVE PASADENA CA 91109
1	NASA LANGLEY RESEARCH CENTER ATTN G B NORTHAM MS 168 LANGLEY STATION HAMPTON VA 23365	1	CALIFORNIA INSTITUTE OF TECHNOLOGY ATTN F E C CULICK MC 301 46 204 KARMAN LAB PASADENA CA 91125
4	NATIONAL BUREAU OF STANDARDS US DEPARTMENT OF COMMERCE ATTN J HASTIE M JACOX T KASHIWAGI H SEMERJIAN WASHINGTON DC 20234	1	UNIVERSITY OF CALIFORNIA LOS ALAMOS SCIENTIFIC LAB P O BOX 1663 MAIL STOP B216 LOS ALAMOS NM 87545
2	DIRECTOR LAWRENCE LIVERMORE NATIONAL LAB ATTN C WESTBROOK W TAO MS L 282 P O BOX 808 LIVERMORE CA 94550	1	UNIVERSITY OF CALIFORNIA BERKELEY CHEMISTRY DEPARMENT ATTN C BRADLEY MOORE 211 LEWIS HALL BERKELEY CA 94720
1	DIRECTOR LOS ALAMOS NATIONAL LAB ATTN B NICHOLS T7 MS B284 P O BOX 1663 LOS ALAMOS NM 87545	1	UNIVERSITY OF CALIFORNIA SAN DIEGO ATTN F A WILLIAMS AMES B010 LA JOLLA CA 92093
1	NATIONAL SCIENCE FOUNDATION ATTN A B HARVEY WASHINGTON DC 20550		

<u>NO. OF COPIES</u>	<u>ORGANIZATION</u>	<u>NO. OF COPIES</u>	<u>ORGANIZATION</u>
2	UNIV OF CALIFORNIA SANTA BARBARA QUANTUM INSTITUTE ATTN K SCHOFIELD M STEINBERG SANTA BARBARA CA 93106	1	THE JOHNS HOPKINS UNIV CPIA ATTN T W CHRISTIAN 10630 LITTLE PATUXENT PKWY SUITE 202 COLUMBIA MD 21044-3200
1	UNIV OF COLORADO AT BOULDER ENGINEERING CENTER ATTN J DAILY CAMPUS BOX 427 BOULDER CO 80309-0427	1	UNIVERSITY OF MICHIGAN GAS DYNAMICS LAB ATTN G M FAETH AEROSPACE ENGINEERING BLDG ANN ARBOR MI 48109-2140
3	UNIV OF SOUTHERN CALIFORNIA DEPT OF CHEMISTRY ATTN R BEAUDET S BENSON C WITTIG LOS ANGELES CA 90007	1	UNIVERSITY OF MINNESOTA DEPT OF MECHANICAL ENGINEERING ATTN E FLETCHER MINNEAPOLIS MN 55455
1	CORNELL UNIVERSITY DEPARTMENT OF CHEMISTRY ATTN T A COOL BAKER LABORATORY ITHACA NY 14853	4	PENNSYLVANIA STATE UNIVERSITY DEPT OF MECHANICAL ENGINEERING ATTN K KUO M MICCI S THYNELL V YANG UNIVERSITY PARK PA 16802
1	UNIVERSITY OF DELAWARE CHEMISTRY DEPARTMENT ATTN T BRILL NEWARK DE 19711	1	POLYTECHNIC INSTITUTE OF NY GRADUATE CENTER ATTN S LEDERMAN ROUTE 110 FARMINGDALE NY 11735
1	UNIVERSITY OF FLORIDA DEPT OF CHEMISTRY ATTN J WINEFORDNER GAINESVILLE FL 32611	2	PRINCETON UNIVERSITY FORRESTAL CAMPUS LIBRARY ATTN K BREZINSKY I GLASSMAN P O BOX 710 PRINCETON NJ 08540
3	GEORGIA INSTITUTE OF TECHNOLOGY SCHOOL OF AEROSPACE ENGINEERING ATTN E PRICE W C STRAHLE B T ZINN ATLANTA GA 30332	1	PURDUE UNIVERSITY SCHL OF AERONAUTICS & ASTRONAUTICS ATTN J R OSBORN GRISCOM HALL WEST LAFAYETTE IN 47906
1	UNIVERSITY OF ILLINOIS DEPT OF MECH ENG ATTN H KRIER 144MEB 1206 W GREEN ST URBANA IL 61801	1	PURDUE UNIVERSITY DEPARTMENT OF CHEMISTRY ATTN E GRANT WEST LAFAYETTE IN 47906

<u>NO. OF COPIES</u>	<u>ORGANIZATION</u>	<u>NO. OF COPIES</u>	<u>ORGANIZATION</u>
2	PURDUE UNIVERSITY SCHL OF MECHANICAL ENGRNG ATTN N M LAURENDEAU S N B MURTHY TSPC CHAFFEE HALL WEST LAFAYETTE IN 47906	1	COHEN PROFESSIONAL SERVICES ATTN N S COHEN 141 CHANNING STREET REDLANDS CA 92373
1	RENSSELAER POLYTECHNIC INST DEPT OF CHEMICAL ENGINEERING ATTN A FONTIJN TROY NY 12181	1	EXXON RESEARCH & ENG CO ATTN A DEAN ROUTE 22E ANNANDALE NJ 08801
1	STANFORD UNIVERSITY DEPT OF MECHANICAL ENGINEERING ATTN R HANSON STANFORD CA 94305	1	GENERAL APPLIED SCIENCE LABS INC 77 RAYNOR AVENUE RONKONKAMA NY 11779-6649
1	UNIVERSITY OF TEXAS DEPT OF CHEMISTRY ATTN W GARDINER AUSTIN TX 78712	1	GENERAL ELECTRIC ORDNANCE SYSTEMS ATTN J MANDZY 100 PLASTICS AVENUE PITTSFIELD MA 01203
1	VA POLYTECH INST AND STATE UNIV ATTN J A SCHETZ BLACKSBURG VA 24061	1	GENERAL MOTORS RSCH LABS PHYSICAL CHEMISTRY DEPARTMENT ATTN T SLOANE WARREN MI 48090-9055
1	APPLIED COMBUSTION TECHNOLOGY INC ATTN A M VARNEY P O BOX 607885 ORLANDO FL 32860	2	HERCULES INC ATTN W B WALKUP E A YOUNT P O BOX 210 ROCKET CENTER WV 26726
2	APPLIED MECHANICS REVIEWS ASME ATTN R E WHITE & A B WENZEL 345 E 47TH STREET NEW YORK NY 10017	1	HERCULES INC ATTN R V CARTWRIGHT 100 HOWARD BLVD KENVIL NJ 07847
1	ATLANTIC RESEARCH CORP ATTN R H W WAESCHE 7511 WELLINGTON ROAD GAINESVILLE VA 22065	1	ALLIANT TECHSYSTEMS INC MARINE SYSTEMS GROUP ATTN D E BRODEN MS MN50 2000 600 2ND STREET NE HOPKINS MN 55343
1	TEXTRON DEFENSE SYSTEMS ATTN A PATRICK 2385 REVERE BEACH PARKWAY EVERETT MA 02149-5900	1	ALLIANT TECHSYSTEMS INC ATTN R E TOMPKINS MN 11 2720 600 SECOND ST NORTH HOPKINS MN 55343
1	BATTELLE TWSTIAC 505 KING AVENUE COLUMBUS OH 43201-2693	1	IBM CORPORATION RESEARCH DIVISION ATTN A C TAM 5600 COTTLE ROAD SAN JOSE CA 95193

<u>NO. OF COPIES</u>	<u>ORGANIZATION</u>	<u>NO. OF COPIES</u>	<u>ORGANIZATION</u>
1	IIT RESEARCH INSTITUTE ATTN R F REMALY 10 WEST 35TH STREET CHICAGO IL 60616	1	SVERDRUP TECHNOLOGY INC LERC GROUP ATTN R J LOCKE MS SVR 2 2001 AEROSPACE PARKWAY BROOK PARK OH 44142
1	LOCKHEED MISSILES & SPACE CO ATTN GEORGE LO 3251 HANOVER STREET DEPT 52 35 B204 2 PALO ALTO CA 94304	1	SVERDRUP TECHNOLOGY INC ATTN J DEUR 2001 AEROSPACE PARKWAY BROOK PARK OH 44142
1	OLIN ORDNANCE ATTN V McDONALD LIBRARY P O BOX 222 ST MARKS FL 32355-0222	3	THIOKOL CORPORATION ELKTON DIVISION ATTN R BIDDLE R WILLER TECH LIB P O BOX 241 ELKTON MD 21921
1	PAUL GOUGH ASSOCIATES INC ATTN P S GOUGH 1048 SOUTH STREET PORTSMOUTH NH 03801-5423	3	THIOKOL CORPORATION WASATCH DIVISION ATTN S J BENNETT P O BOX 524 BRIGHAM CITY UT 84302
1	HUGHES AIRCRAFT COMPANY ATTN T E WARD 8433 FALLBROOK AVENUE CANOGA PARK CA 91303	1	UNITED TECHNOLOGIES RSCH CENTER ATTN A C ECKBRETH EAST HARTFORD CT 06108
1	ROCKWELL INTERNATIONAL CORP ROCKETDYNE DIVISION ATTN J E FLANAGAN HB02 6633 CANOGA AVENUE CANOGA PARK CA 91304	1	UNITED TECHNOLOGIES CORP CHEMICAL SYSTEMS DIVISION ATTN R R MILLER P O BOX 49028 SAN JOSE CA 95161-9028
1	SCIENCE APPLICATIONS INC ATTN R B EDELMAN 23146 CUMORAH CREST WOODLAND HILLS CA 91364	1	UNIVERSAL PROPULSION COMPANY ATTN H J MCSPADDEN 25401 NORTH CENTRAL AVENUE PHOENIX AZ 85027-7837
3	SRI INTERNATIONAL ATTN G SMITH D CROSLEY D GOLDEN 333 RAVENSWOOD AVENUE MENLO PARK CA 94025	1	VERITAY TECHNOLOGY INC ATTN E B FISHER 4845 MILLERSPORT HIGHWAY EAST AMHERST NY 14051-0305
1	STEVENS INSTITUTE OF TECH DAVIDSON LABORATORY ATTN R MCALEVY III HOBOKEN NJ 07030	1	FREEDMAN ASSOCIATES ATTN E FREEDMAN 2411 DIANA ROAD BALTIMORE MD 21209-1525

<u>NO. OF COPIES</u>	<u>ORGANIZATION</u>	<u>NO. OF COPIES</u>	<u>ORGANIZATION</u>
6	ALLIANT TECHSYSTEMS ATTN C CANDLAND L OSGOOD R BECKER J BODE R BURETTA M SWENSON 600 SECOND ST NE HOPKINS MN 55343	35	<u>ABERDEEN PROVING GROUND</u> DIR USARL ATTN: AMSRL-WM-P, A HORST AMSRL-WM-PC, B E FORCH G F ADAMS W R ANDERSON R A BEYER S W BUNTE C F CHABALOWSKI K P MCNEILL-BOONSTOPPEL A COHEN R CUMPTON R DANIEL D DEVYNCK N F FELL J M HEIMERL A J KOTLAR M R MANAA W F MCBRATNEY K L MCNESBY S V MEDLIN M S MILLER A W MIZOLEK S H MODIANO J B MORRIS J E NEWBERRY S A NEWTON R A PESCE-RODRIGUEZ B M RICE R C SAUSA M A SCHROEDER J A VANDERHOFF M WENSING A WHREN J M WIDDER C WILLIAMSON AMSRL-CI-CA, R PATEL
1	DIRECTOR US ARMY BENET LABS ATTN AMSTA AR CCB T SAM SOPOK WATERVLIET NY 12189		

INTENTIONALLY LEFT BLANK.

REPORT DOCUMENTATION PAGE

*Form Approved
OMB No. 0704-0188*

Public reporting burden for this collection of information is estimated to average 1 hour per response, including the time for reviewing instructions, searching existing data sources, gathering and maintaining the data needed, and completing and reviewing the collection of information. Send comments regarding this burden estimate or any other aspect of this collection of information, including suggestions for reducing this burden, to Washington Headquarters Services, Directorate for Information Operations and Reports, 1215 Jefferson Davis Highway, Suite 1204, Arlington, VA 22202-4302, and to the Office of Management and Budget, Paperwork Reduction Project(0704-0188), Washington, DC 20503.

1. AGENCY USE ONLY <i>(Leave blank)</i>	2. REPORT DATE	3. REPORT TYPE AND DATES COVERED	
	March 1997	Final, June 1995 - June 1996	
4. TITLE AND SUBTITLE		5. FUNDING NUMBERS	
Spectroscopic Determination of Impact Sensitivities of Explosives		PR: 1L161102AH43	
6. AUTHOR(S)			
K. L. McNesby and C. S. Coffey*			
7. PERFORMING ORGANIZATION NAME(S) AND ADDRESS(ES)		8. PERFORMING ORGANIZATION REPORT NUMBER	
U.S. Army Research Laboratory ATTN: AMSRL-WM-PC Aberdeen Proving Ground, MD 21005-5066		ARL-TR-1323	
9. SPONSORING/MONITORING AGENCY NAMES(S) AND ADDRESS(ES)		10. SPONSORING/MONITORING AGENCY REPORT NUMBER	
11. SUPPLEMENTARY NOTES			
* C. S. Coffey is from the Naval Surface Warfare Center, Silver Spring, MD 20903-5000.			
12a. DISTRIBUTION/AVAILABILITY STATEMENT		12b. DISTRIBUTION CODE	
Approved for public release; distribution is unlimited.			
13. ABSTRACT <i>(Maximum 200 words)</i>			
A simple theory is developed that predicts impact sensitivities in crystalline explosives from vibrational spectra measured at room temperature. The theory uses Raman spectra of energetic materials to construct vibrational energy level diagrams, which are then used as input for a model designed to calculate the rate of energy transfer from phonon and near-phonon vibrational energy levels to higher energy vibrational levels. Energy transfer rates are determined using Fermi's Golden Rule, and results from simple theories of near-resonant energy transfer. The application of the theory and model, using Raman spectra of seven different neat explosive samples, gives results in good agreement with results of drop weight impact tests.			
14. SUBJECT TERMS		15. NUMBER OF PAGES	
explosive initiation, vibrational energy transfer, Raman spectroscopy		42	
		16. PRICE CODE	
17. SECURITY CLASSIFICATION OF REPORT	18. SECURITY CLASSIFICATION OF THIS PAGE	19. SECURITY CLASSIFICATION OF ABSTRACT	20. LIMITATION OF ABSTRACT
UNCLASSIFIED	UNCLASSIFIED	UNCLASSIFIED	UL

INTENTIONALLY LEFT BLANK.

USER EVALUATION SHEET/CHANGE OF ADDRESS

This Laboratory undertakes a continuing effort to improve the quality of the reports it publishes. Your comments/answers to the items/questions below will aid us in our efforts.

1. ARL Report Number/Author ARL-TR-1323 (McNesby) Date of Report March 1997

2. Date Report Received _____

3. Does this report satisfy a need? (Comment on purpose, related project, or other area of interest for which the report will be used.)

4. Specifically, how is the report being used? (Information source, design data, procedure, source of ideas, etc.)

5. Has the information in this report led to any quantitative savings as far as man-hours or dollars saved, operating costs avoided, or efficiencies achieved, etc? If so, please elaborate.

6. General Comments. What do you think should be changed to improve future reports? (Indicate changes to organization, technical content, format, etc.)

Organization _____

CURRENT
ADDRESS

Name _____ E-mail Name _____

Street or P.O. Box No. _____

City, State, Zip Code _____

7. If indicating a Change of Address or Address Correction, please provide the Current or Correct address above and the Old or Incorrect address below.

Organization _____

OLD
ADDRESS

Name _____

Street or P.O. Box No. _____

City, State, Zip Code _____

(Remove this sheet, fold as indicated, tape closed, and mail.)
(DO NOT STAPLE)

DEPARTMENT OF THE ARMY

OFFICIAL BUSINESS

BUSINESS REPLY MAIL
FIRST CLASS PERMIT NO 0001, APG, MD

POSTAGE WILL BE PAID BY ADDRESSEE

DIRECTOR
US ARMY RESEARCH LABORATORY
ATTN AMSRL WM PC
ABERDEEN PROVING GROUND MD 21005-5066



**NO POSTAGE
NECESSARY
IF MAILED
IN THE
UNITED STATES**

